**ENGINEERING
FAILURE
ANALYSIS**

ELSEVIER

Thermal stress for all-ceramics rolls used in molten metal to produce stable high quality galvanized steel sheet

Nao-Aki Noda [a,*], Masahiro Yamada [a], Yoshikazu Sano [b],
Shigetada Sugiyama [b], Shoichi Kobayashi [c]

[a] *Kyushu Institute of Technology, Department of Mechanical Engineering, 1-1, Sensui-cho, Tobata, Kitakyushu 804-8550, Japan*
[b] *Hitachi Metals, Wakamatsu Works, 1-9-1, Kitahama, Wakamatsu, Kitakyushu 808-0043, Japan*
[c] *Nittetsu Plant Designing Corporation, 1-9-1, Nakabaru, Tobata, Kitakyushu 808-0002, Japan*

Abstract

The zinc coated steel sheet has been mostly used for automobile and other industries because of its high corrosion resistance. This paper deals with the development of new ceramics support roll used for a continuous galvanizing pot to manufacture stable galvanizing steel sheet. Usually stainless steel rolls coated by tungsten carbide are used to support and stabilize the strip in a continuous galvanizing pot, which is filled with molten zinc. However, corrosion and abrasion arise on the roll surface only in a few weeks, and causing the deterioration of quality of plating. Although developing all-ceramics rolls is most desirable, risk of fracture has to be reduced when the ceramic roll dips into molten metal. In this paper, therefore, how to reduce the thermal stress is considered when the ceramic rolls are installed in molten metal using finite volume method and finite element method. The usefulness of silicon nitride having extremely high conductivity is also discussed.
© 2007 Elsevier Ltd. All rights reserved.

1. Introduction

The zinc coated steel sheet has been used for automobiles, refrigerators, and washing machines etc. because of its high corrosion resistance [1]. In recent years, several continuous galvanizing lines are constructing to meet the demand for those industries. To improve the quality of plating strips, automation technologies to control the zinc coating thickness and galvannealing were considered [2,3]. Fig. 1 shows the layout of a continuous galvanizing line [1–6]. Strip coils rolled by the cold rolling mill are automatically mounted on the pay-off reel. After subsequent welding, the strip is passed through an automatically controlled annealing furnace to be heated to a specific temperature, and then dipped in a zinc bath through a protective gas atmosphere. In the

---

* Corresponding author. Tel./fax: +81 93 884 3124.
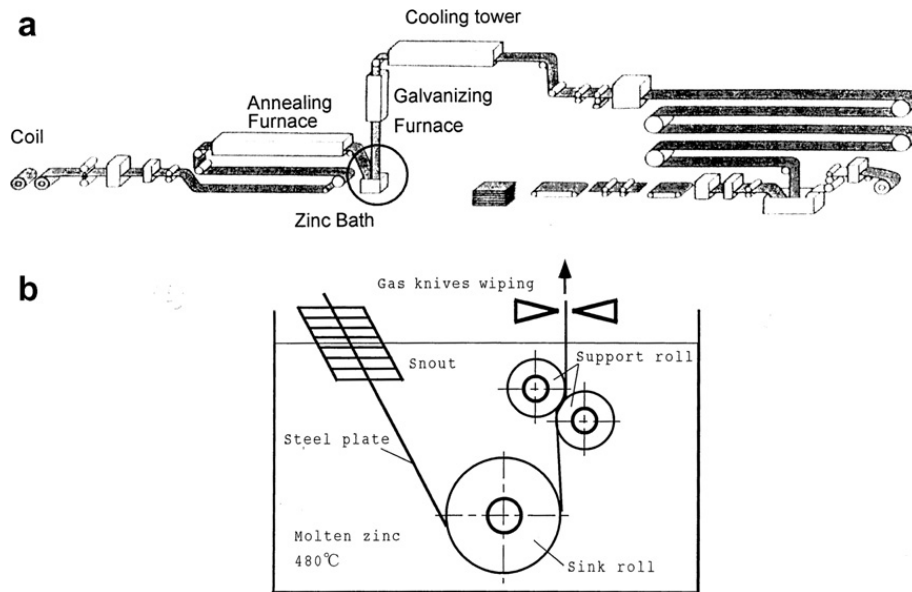 *E-mail address:* noda@mech.kyutech.ac.jp (N.-A. Noda).

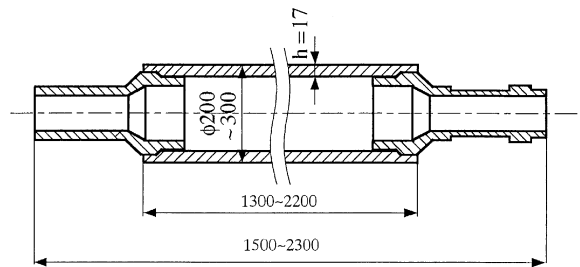Fig. 1. (a) Layout of continuous galvanizing line; (b) detail of zinc bath.

Fig. 2. All-ceramics support roll.

molten zinc bath, the strip changes the direction by the sink roll; after rectifying the warping of the plate by a pair of support rolls, the steel sheet is withdrawn from the pot. A wiping nozzle provided immediately above the zinc bath sandwiches the strip, and controls the zinc coating thickness to the specified value by the discharged gas. With galvanneald steel, the coated strip is heated in the galvannealing furnace, where the degree of alloying between the zinc coating layer and substrate is controlled. After passing through the temper mill and tension leveler, the strip is subjected to chromate treatment and oiling, and cut into suitable sized sheets.

In the molten zinc bath, the sink rolls and the support rolls are usually made of stainless steel [7–9]; however, since the molten zinc has a high temperature 480 °C, corrosion and abrasion arise on the roll surface only in a few weeks, and causing the deterioration of quality of plating. Therefore, every two or three weeks, continuous galvanizing lines must stop to change the rolls. Thanks to its excellent high-temperature strength, all-ceramics rolls as shown in Fig. 2 have attracted much attention [7]. However, risk of fracture has to be reduced when the ceramic roll dips into molten metal and operates. In this paper, therefore, how to reduce the thermal stress will be considered when the all-ceramics rolls are installed in molten metal using finite element method. The use of special silicon nitride that has extremely high thermal conductivity [10] will be also considered to reduce the thermal stress. It should be noted that those thermal stresses are harmless for stainless steels, but possibly harmful for ceramics because of low fracture toughness.

2. Previous studies for sink and support rolls used in molten zinc

In the molten zinc bath in Fig. 1b, the sink roll has 500–800 mm in diameter, and 1300–2200 mm in length. The support rolls has 200–350 mm in diameter, and 1300–2200 mm in length. They are usually made of stainless steel because of the highest corrosion resistance among all kinds of metals. To improve the corrosion resis-
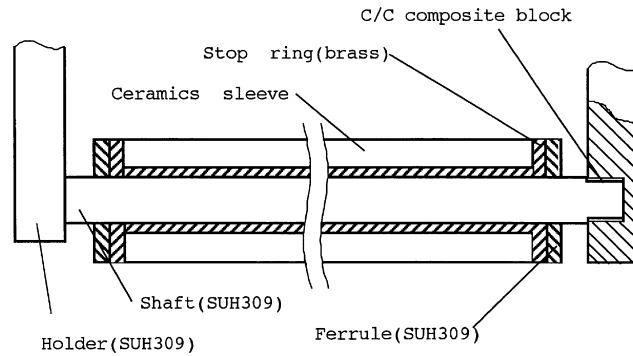
Fig. 3. Ceramics sleeve with a shaft made of heat resisting steel SUH309.

tance, tungsten carbide is usually sprayed on the roll surface, and cobalt-based alloy is sometimes welded on the surface [7,8]. However, cracks appear easily in the vicinity of the interface owing to the difference of the thermal expansion ratio between the two metals.

Fig. 3 shows an example of the roll previously developed using a ceramics sleeve with a shaft made of heat resisting steel SUH309 [9]. Since the thermal expansion ratio of the shaft is higher than the one of the sleeve, there is risk of fracture when the roll is put into the zinc bath. Also corrosion appears on the stop ring and shaft because they are still made of metals. Moreover, the roll cannot rotate smoothly in accordance with the movement of the strip because of too much weight. From those experience, all-ceramics roll as shown in Fig. 2 is known to be desirable for support rolls used in the zinc bath [4–7].

3. Evaluation for surface heat transfer

To calculate the thermal stress, it is necessary to know the surface heat transfer α when the ceramics roll dips into the molten zinc. Since three-dimensional thermo-fluid analysis to estimate α is very complicated,

Table 1
The physical property of molten zinc at 693 K (420 °C) [13]

Thermal conductivity (λ (W/m K))	58.8
Roll diameter (D (m))	0.250
Constants in Eq. (1) when $Re = 1 \times 10^3$–2×10^5 (C_1)	0.26
Constants in Eq. (1) when $Re = 1 \times 10^3$–2×10^5 (n)	0.6
Kinematic viscosity (v (mm^2/s))	0.489
Isobaric specific heat (C_p (kJ/kg K))	0.505
Viscosity (η (mPa s))	3.26

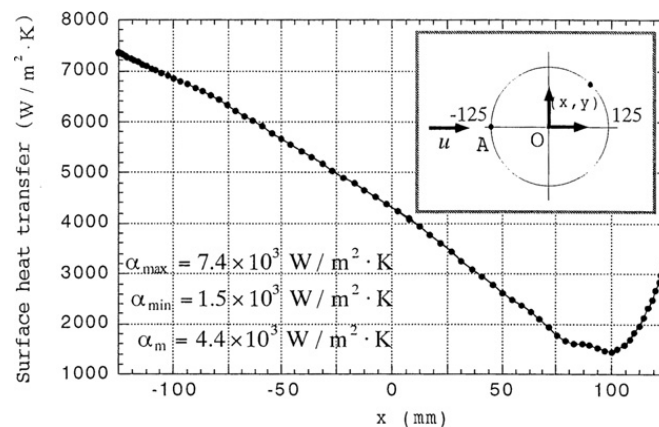Fig. 4. Surface heat transfer as a function of x ($u = 25$ mm/s).

two-dimensional (2-D) solution will be considered. Zukauskas [11,12] proposed the following equation to estimate Nusselt number when a two-dimensional cylinder in the fluid with the velocity u.

$$Nu_m \equiv \frac{\alpha_m D}{\lambda} = C_1 Re^n Pr^{0.37} \left(\frac{Pr}{Pr_w}\right)^{0.25} \tag{1}$$

Here, α_m is the average heat transfer coefficient, λ is thermal conductivity, D is a diameter of a cylinder, C_1, n are constants determined from Reynolds number [2,3]. Also, Re is Reynolds number, Pr is Prandtl number, subscript w denotes the property for the temperature of the cylinder wall.

$$Re = \frac{uD}{v}, \quad Pr = \frac{C_P \cdot \eta}{\lambda} \tag{2}$$

Here, velocity u can be calculated by the diameter of the roll divided by the time when the cylinder dips into the zinc, which is usually, $u = 25\text{--}2$ mm/s. The values of kinematic velocity v, isobaric specific heat C_p, viscosity η are given from the reference [3] and shown in Table 1. Substituting these into Eqs. (1) and (2), Nu_m is given from α_m. Namely,

$$\alpha_m = 1.0 \times 10^3 \text{ W/m}^2 \text{ K} \quad (\text{when } u = 2 \text{ mm/s}) \tag{3}$$

Table 2
Mechanical properties of ceramics

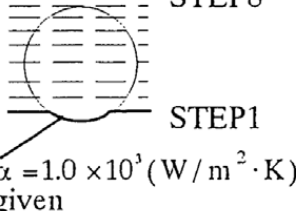| Physical property (dimension)	Sialon	Silicon nitride
Thermal conductivity (W/m K)	17	65
Specific heat (J/kg K)	650	680
Coefficient of linear expansion (1/K)	3.0×10^{-6}	3.0×10^{-6}
Young's modulus (GPa (Kgf/mm^2))	294 (29,979)	300 (30,591)
Specific weight	3.26	3.20
Poisson's ratio	0.27	0.30
4 Point bending strength (MPa (Kgf/mm^2))	1050 (10,296)	880 (8630)
Fracture toughness (MN/m$^{3/2}$)	7.5	7.7
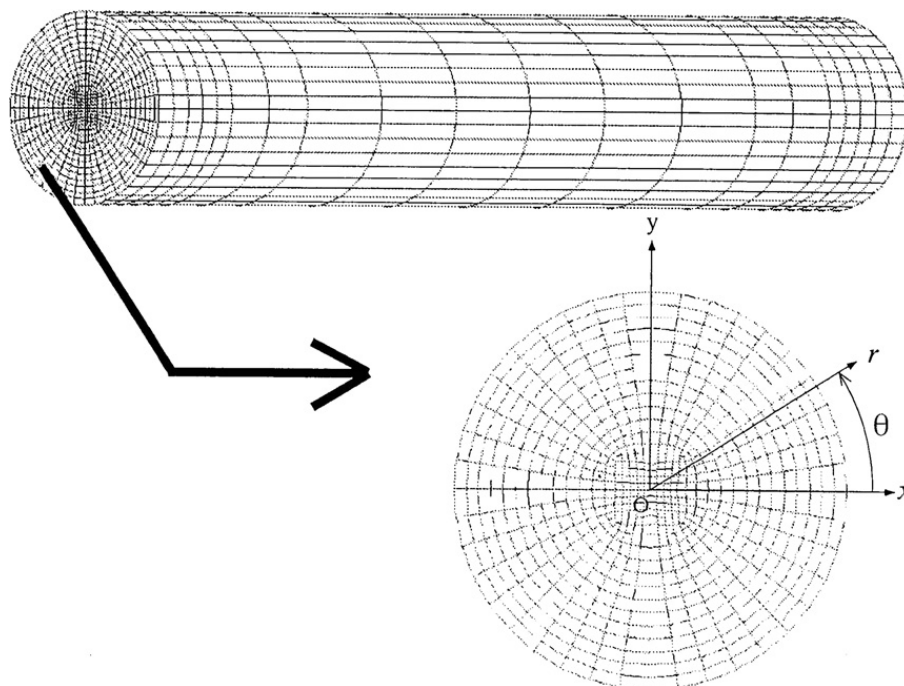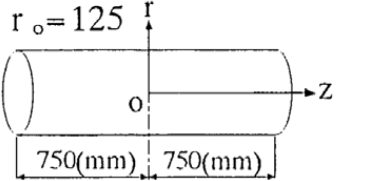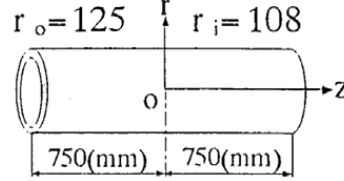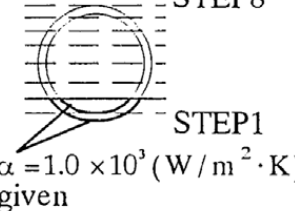
Fig. 5. Finite element mesh (number of element = 13,200, number of nodes = 14,301).

$$\alpha_m = 4.6 \times 10^3 \ \text{W/m}^2 \ \text{K} \quad \text{(when } u = 25 \text{ mm/s)} \tag{4}$$

Next, to calculate the heat transfer more accurately, the finite volume method is applied to the static 2-D heat transfer model. Here, the roll is fixed, and the fluid velocity is assumed $u = 25$ mm/s. In this analysis, the hexa-

Table 3
Assumption of heat transfer α

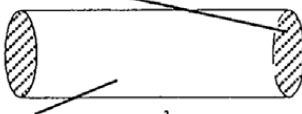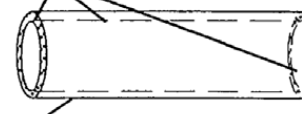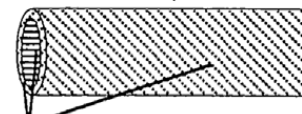| Model	(a) Solid cylinder $r_o = 125$	(b) Hollow cylinder $r_o = 125$, $r_i = 108$
$u = 2$ mm/s	$z = \pm 750 \text{(mm)}$ $r = 125 \text{(mm)}$ $\alpha = 1.0 \times 10^3 (\text{W}/\text{m}^2 \cdot \text{K})$ STEP8 STEP1 $\alpha = 1.0 \times 10^3 (\text{W}/\text{m}^2 \cdot \text{K})$ given	$z = \pm 750 \text{(mm)}$ $r = 125 \text{(mm)}$ $\alpha = 1.0 \times 10^3 (\text{W}/\text{m}^2 \cdot \text{K})$ STEP8 STEP1 $\alpha = 1.0 \times 10^3 (\text{W}/\text{m}^2 \cdot \text{K})$ given
$u = 25$ mm/s	(1)t=0~30sec $z = \pm 750 \text{(mm)}$ $\alpha = 1.5 \times 10^3 (\text{W}/\text{m}^2 \cdot \text{K})$ $r = 125 \text{(mm)}$ $\alpha = 1.5 \times 10^3 \sim 7.0 \times 10^3$ $(\text{W}/\text{m}^2 \cdot \text{K})$ (see Fig.4) $\alpha = 1.5 \times 10^3 (\text{W}/\text{m}^2 \cdot \text{K})$ $\alpha = 1.5 \times 10^3 \sim 7.0 \times 10^3$ $(\text{W}/\text{m}^2 \cdot \text{K})$(see Fig.4) (2)t=30~120sec $z = \pm 750 \text{(mm)}$ $r = 125 \text{(mm)}$ $\alpha = 1.5 \times 10^3 (\text{W}/\text{m}^2 \cdot \text{K})$ $\alpha = 1.5 \times 10^3 (\text{W}/\text{m}^2 \cdot \text{K})$	(1)t=0~30sec $z = \pm 750 \text{(mm)}$ $\alpha = 1.5 \times 10^3 (\text{W}/\text{m}^2 \cdot \text{K})$ $r = 125 \text{(mm)}$ $\alpha = 1.5 \times 10^3 \sim 7.0 \times 10^3$ $(\text{W}/\text{m}^2 \cdot \text{K})$ (see Fig.4) $r = 108 \text{(mm)}$ $\alpha = 1.5 \times 10^3 (\text{W}/\text{m}^2 \cdot \text{K})$ $\alpha = 1.5 \times 10^3 (\text{W}/\text{m}^2 \cdot \text{K})$ $\alpha = 1.5 \times 10^3 \sim 7.0 \times 10^3$ $(\text{W}/\text{m}^2 \cdot \text{K})$(see Fig.4) (2)t=30~120sec $z = \pm 750 \text{(mm)}$ $r = 125 \text{(mm)}$ $r = 108 \text{(mm)}$ $\alpha = 1.5 \times 10^3 (\text{W}/\text{m}^2 \cdot \text{K})$ $\alpha = 1.5 \times 10^3 (\text{W}/\text{m}^2 \cdot \text{K})$

hedral mesh is used; then, RNG k-ε as turbulence model, first order UP-Wind as convective term, and SIMPLE algorithm as pressure-velocity coupling are applied.

The calculation results are shown in Fig. 4. The maximum heat transfer $\alpha = 7.4 \times 10^3$ W/m^2 K appears at $x = -125$ mm, the minimum value $\alpha = 1.5 \times 10^3$ W/m^2 K appears at $x = 100$ mm. The average value is $\alpha_m = 4.4 \times 10^3$ W/m^2 K, which is in good agreement with Eq. (4).

4. The results of thermal stress

Table 2 shows mechanical properties of ceramics. Here, two kinds of ceramics are considered; one is sialon, which was developed as a suitable material for large ceramic structures [4–6]. The other is a special silicon nitride whose thermal conductivity is extremely high [10]. As shown in Table 2, the thermal conductivity of the special silicon nitride is larger than the one of the sialon by 3.8 times. Eight nodes three-dimensional elements will be employed. Currently, a hollow cylinder as shown in Fig. 2 seems desirable, but details of the cylinder dimensions will be changed in the future to meet the new demands. Therefore in this paper two simplified models will be considered; one is a simple solid cylinder, and the other is a simple hollow cylinder (see Figs. 5 and 8). The temperature of the molten zinc is assumed at 480 °C, and the initial temperature of the roll is assumed 20 °C except for the discussion at the Section 4.5.

4.1. The thermal stress for solid cylinder dipping slowly u = 2 mm/s

First, a solid cylinder model as shown in Fig. 5 is considered when the cylinder dips into molten zinc slowly, $u = 2$ mm/s. Here, a total of 13,200 elements with 14,301 nodes have been used. When $u = 2$ mm/s, $\alpha_m = 1.0 \times 10^3$ W/m^2 K as shown in Eq. (3) is applied for all the surfaces, $r = 125$ mm and $z = \pm 750$ mm. Since it takes 120 s before completely dipping, eight kinds of partially dipping models are considered as shown in Table 3, and $\alpha_m = 1.0 \times 10^3$ W/m^2 K is applied to the surface touching molten zinc. Then, the results are shown in Fig. 6. Fig. 6 indicates the maximum tensile principle stress σ_1, maximum compressive principle stress σ_3, and maximum stresses components σ_r, σ_θ, σ_z. Since the maximum shear stresses τ_{rz}, $\tau_{\theta z}$, $\tau_{r\theta}$ are within 27% of $\sigma_{z\max}$, only the largest shear stress τ_{rz} is indicated. From Fig. 6 it is seen that $\sigma_{z\max}$ coincides with σ_1 at $t = 75$ s, and $\sigma_{z\min}$ coincides with σ_3 at $t = 114$ s. In the following figures, therefore, only $\sigma_{z\max}$, $\sigma_{z\min}$ will be discussed because they are almost equivalent to the maximum stresses σ_1, σ_3, respectively. The stress $\sigma_{z\max}$ has the peak value of 156 MPa at 143 s.

4.2. The thermal stress for solid cylinder dipping fast u = 25 mm/s

Next, the thermal stress is considered when the solid cylinder in Fig. 5 dips into molten zinc fast, $u = 25$ mm/s. In this case the whole part of the roll is assumed in the zinc because it takes only 10 s to dip
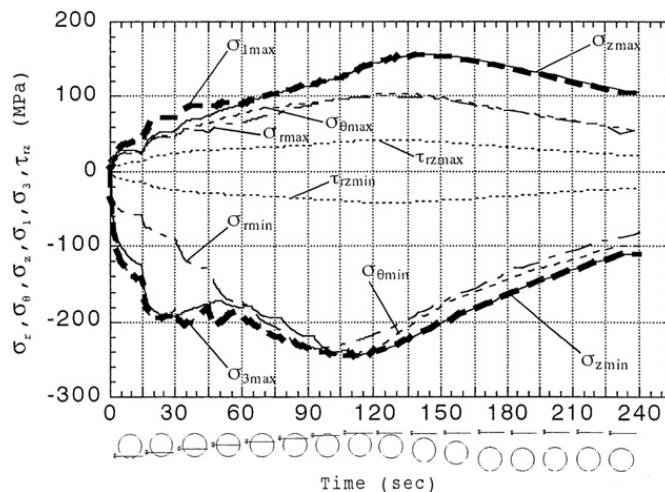

Fig. 6. Maximum stresses σ_r, σ_θ, σ_z, σ_1, σ_3, τ_{rz} vs. time relation for solid cylinder made of special silicon nitride ($u = 2$ mm/s).

into the bath, and 16 s to the roll position (see Fig. 1b). It should be noted that the molten zinc is still in motion even after the cylinder is installed in the zinc bath. Therefore, the surface heat transfer is assumed in the following way.

(1) When $t = 0$–30 s, $\alpha = (7.4$–$1.5) \times 10^3$ W/m^2 K as shown in Fig. 4 is applied at the cylinder surface, $r = 125$ mm; and also $\alpha = 1.5 \times 10^3$ W/m^2 K, which is the minimum value in Fig. 4, is assumed at the cylinder end, $z = \pm 750$ mm.
(2) When $t > 30$ s, $\alpha = 1.5 \times 10^3$ W/m^2 K is assumed for whole the surface. Then, the results are shown in Fig. 7.

In Fig. 7, it is seen that the maximum stresses σ_{zmax} increases in a short time, and has a peak value 185 MPa at $t = 38$ s. Namely, the larger stress appears shortly compared with the case of $u = 2$ mm/s in Fig. 6. It may be concluded that for solid cylinders should dip into slowly in order to reduce the thermal stresses. Actually, in several continuous galvanizing lines the prototypical ceramics rolls are installed in the bath slowly, about $u = 2$ mm/s.
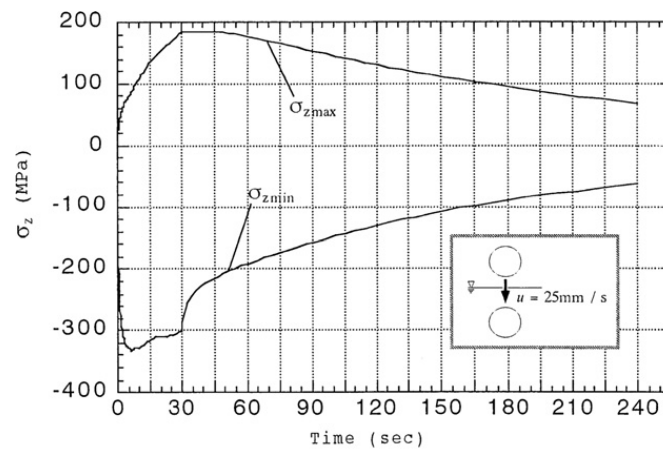

Fig. 7. σ_z vs. time relation for solid cylinder made of special silicon nitride ($u = 25$ mm/s).
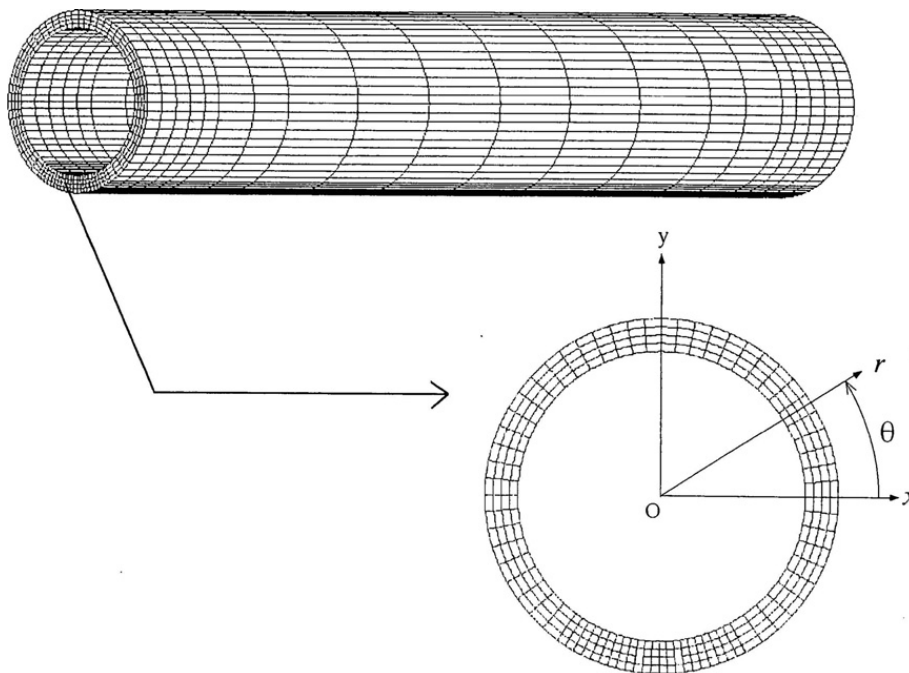

Fig. 8. Finite element mesh (number of element = 5680, number of nodes = 7455).

4.3. The thermal stress for hollow cylinder dipping slowly u = 2 mm/s

Next, a hollow cylinder model as shown in Fig. 8 is considered when the cylinder dips into molten zinc slowly, $u = 2$ mm/s. Here, a total of 5680 elements with 7455 nodes have been used. When $u = 2$ mm/s, $\alpha_m = 1.0 \times 10^3$ W/m^2 K as shown in Eq. (3) is applied for all the surfaces, $r = 125$ mm, $r = 108$ mm, and $z = \pm 750$ mm. Namely, eight kinds of partially dipping models are employed as shown in Table 3, and $\alpha_m = 1.0 \times 10^3$ W/m^2 K is applied to the surface touching molten zinc. Then, the results are indicated as solid lines in Fig. 9. As shown in Fig. 9, σ_{zmax} increases slowly and has a peak value 136 MPa at 17 s. From the comparison between the results of hollow and solid cylinders (see Fig. 9 and 6), it is seen that the maximum stresses are not very different, that is, 136 MPa in Fig. 9 and 156 MPa in Fig. 6. However, in Fig. 9, the maximum value appears very shortly at $t = 17$ s compared with at $t = 143$ s in Fig. 6. In Fig. 9, at $t = 120$ s all thermal stresses almost disappear, and less than 0.1% of the maximum stress. In other words, for hollow cylinders, the thermal stress should be considered only at the beginning of $t = 1$–30 s.

4.4. The thermal stress for hollow cylinder dipping fast u = 25 mm/s

When the hollow cylinder in Fig. 5 dips into fast, $u = 25$ mm/s, the whole cylinder is assumed in the zinc because it takes only 10 s to dip into the bath, and 16 s to the roll position (see Fig. 1b). Similarly to the case of the solid cylinder, the surface heat transfer is assumed in the following way (see Table 3).

(1) When $t = 0$–30 s, $\alpha = (7.4–1.5) \times 10^3$ W/m^2 K as shown in Fig. 4 is applied at the cylinder surface, $r = 125$ mm, $r = 108$ mm; and also $\alpha = 1.5 \times 10^3$ W/m^2 K, which is the minimum value in Fig. 4, is assumed at the cylinder end, $z = \pm 750$ mm.
(2) When $t > 30$ s, $\alpha = 1.5 \times 10^3$ W/m^2 K is assumed for whole the surface. Then, the results are shown in Fig. 10. As shown in Fig. 10, σ_{zmax} increases rapidly, and has a peak value 84 MPa at 0.27 s. Only at $t = 10$ s σ_{zmax} becomes very small, and less than 1.2% of the peak value. From the comparison between Figs. 9 and 10, it should be noted that $\sigma_{zmax} = 84$ MPa at $t = 0.27$ s in Fig. 10 is smaller than
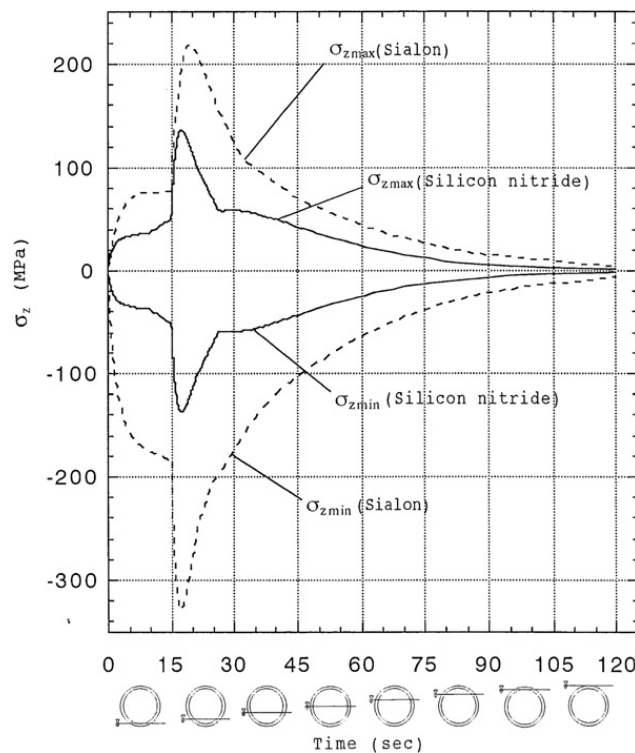

Fig. 9. σ_z vs. time relation for hollow cylinder made of special silicon nitride and sialon ($u = 2$ mm/s).

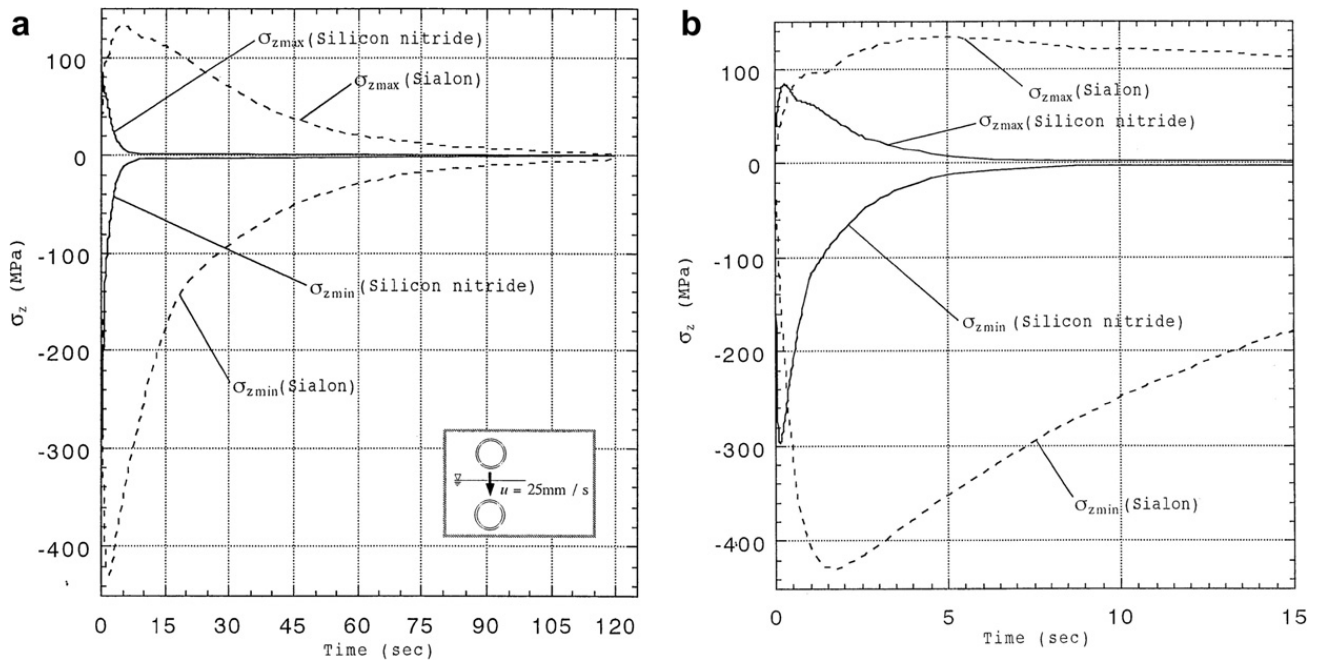Fig. 10. σ_z vs. time relation for hollow cylinder made of special silicon nitride and sialon ($u = 25$ mm/s).

$\sigma_{zmax} = 136$ MPa in Fig. 9 by 38%. Therefore a hollow cylinder should dip fast $u = 25$ mm/s rather than slowly $u = 2$ mm/s to reduce the thermal stresses. In other words, although in several continuous galvanizing lines the hollow rolls are usually set slowly about $u = 2$ mm/s, that is not suitable for reducing the thermal stress.

Fig. 11 shows temperature and stress distributions at the time 17 s and at the section $z = \pm720$ mm where the maximum stress $\sigma_{zmax} = 136$ MPa appears when the hollow cylinder dips slowly (see Fig. 9). The maximum stress appears at the point just above the level of molten zinc. Fig. 12 shows temperature and stress distributions at the time $t = 0.27$ s and at the section $z = \pm630$ mm where the maximum stress $\sigma_{zmax} = 84$ MPa appears when the hollow cylinder dips fast (see Fig. 10). The maximum stress appears closer to the inner surface because larger heat transfer is provided from outer surface.
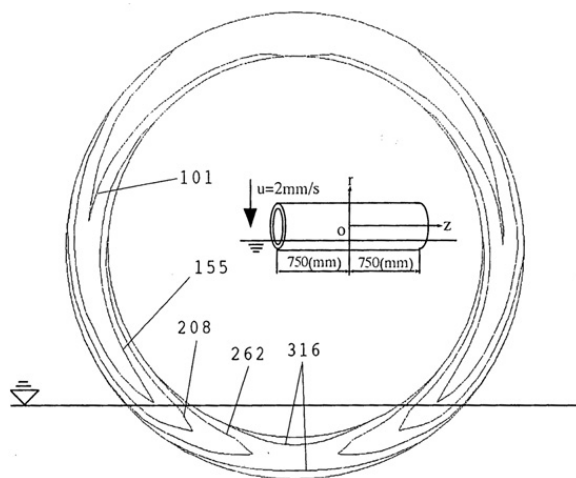

Fig. 11a. Temperature (°C) for special silicon nitride at the time 17 s and at the section $z = \pm720$ mm where the maximum stress $\sigma_{zmax} = 136$ MPa appears ($u = 2$ mm/s, see Fig. 9)

Fig. 11b. Stress σ_z(MPa) for special silicon nitride at time 17 s and at the section $z = \pm720$ mm where the maximum stress $\sigma_{zmax} = 136$ MPa appears ($u = 2$ mm/s, see Fig. 9).

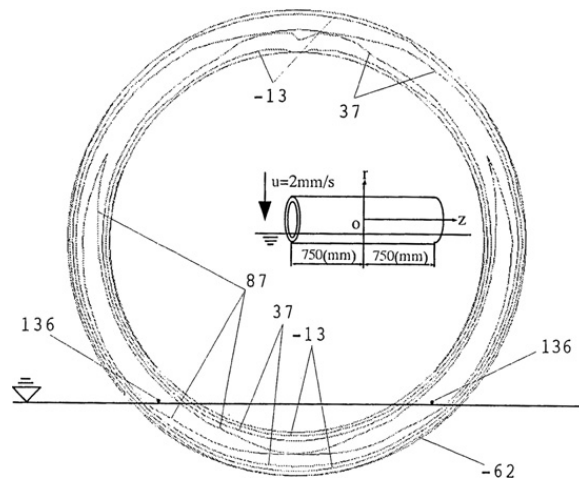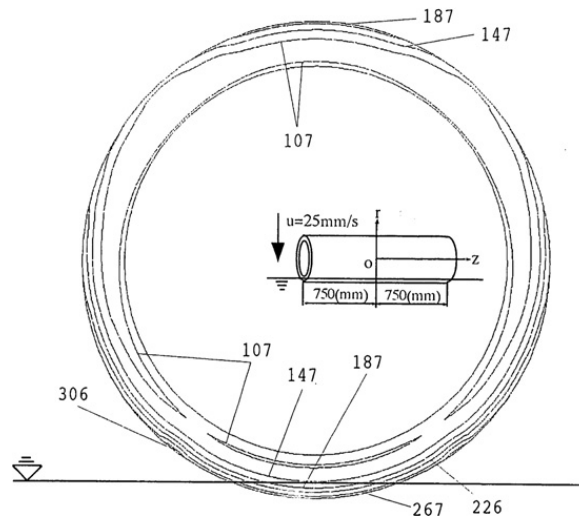Fig. 12a. Temperature (°C) for special silicon nitride at the time $t = 0.27$ s and at the section $z = \pm630$ mm where the maximum stress $\sigma_{zmax} = 84$ MPa appears ($u = 25$ mm/s, see Fig. 10).

4.5. Comparison between the results of sialon and special silicon nitride

Sialon ceramics were developed for the use of large structures under high temperature [4–6]. It was used for thermocouple protective tubes, stalks in the low-pressure diecasting machine, immersion heater tubes, shot sleeve for diecasting, and roll bearing for continuous galvanizing bath [6]. Prototypical all-ceramics support rolls were also manufactured by this sialon. On the other hand, special silicon nitride, which has very high thermal conductivity, was developed for the members for electronic parts, such as a substrate for semi-conductors, a heat sink for heater elements, and a member for molten metal [10]. Since the thermal conductivity of the special silicon nitride is higher than the one of sialon by 3.8 times, the thermal stress may be reduced by the use of this ceramics.

The results of sialon are also indicated in Fig. 9 as dotted lines when the roll dips into slowly $u = 2$ mm/s. The thermal stress has a peak value 219 MPa at $t = 19$ s, which is higher than the value of the special silicon nitride by 61%. It is found that the thermal stress can be reduced by the use of the special silicon nitride by about 40%. Fig. 13 indicates temperature and stress distributions at the time $t = 19$ s and at the section
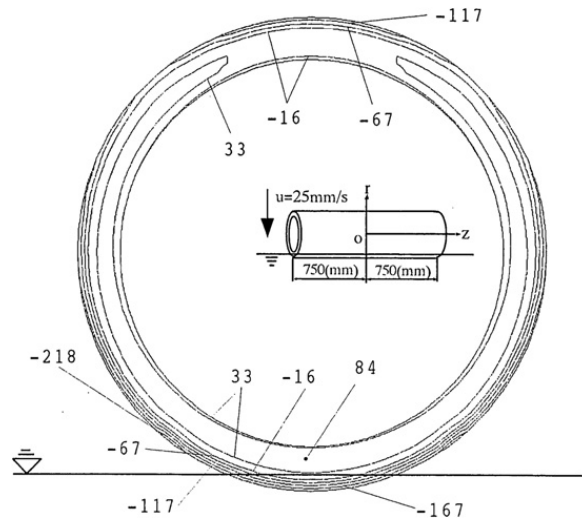
Fig. 12b. Stress σ_z(MPa) for special silicon nitride at the time $t = 0.27$ s and at the section $z = \pm630$ mm where the maximum stress $\sigma_{z\max} = 84$ MPa appears ($u = 25$ mm/s, see Fig. 10).
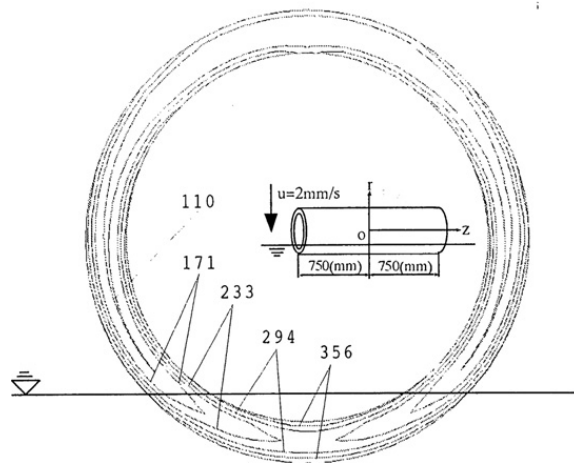

Fig. 13a. Temperature (°C) for hollow cylinder made of sialon at the time $t = 19$ s and at the section $z = \pm720$ mm where the maximum stress $\sigma_{z\max} = 219$ MPa appears ($u = 2$ mm/s, see Fig. 9).

Fig. 13b. Stress σ_z(MPa) for hollow cylinder made of sialon at the time $t = 19$ s and at the section $z = \pm720$ mm where the maximum stress $\sigma_{z\max} = 219$ MPa appears ($u = 2$ mm/s, see Fig. 9).
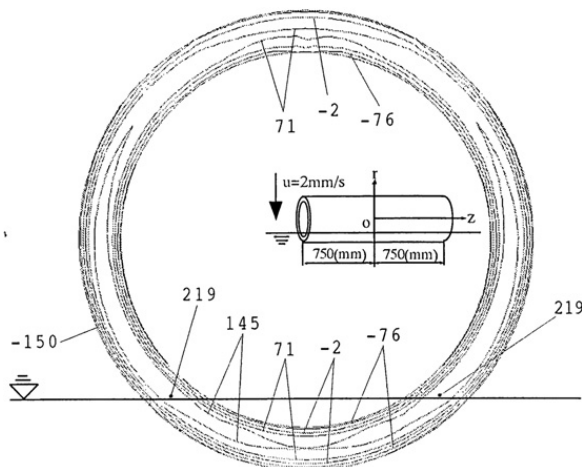
$z = \pm720$ mm where the maximum stress $\sigma_{zmax} = 219$ MPa appears when the hollow cylinder made of sialon dips slowly (see Fig. 9). In Fig. 13a, the temperature difference is significant in the thickness direction compared with the case of Fig. 11a. Lower thermal conductivity of sialon may cause this difference and the higher thermal stress σ_{zmax} as shown in Fig. 13b.

As shown in Fig. 10, when the roll dips fast, the thermal stress of sialon is very different from the one of special silicon nitride. For special silicon nitride only 15 s is necessary for no thermal stress. However, for sialon more than two minutes is necessary. The maximum stress of sialon is higher than the one of special silicon nitride by 58%. From the comparison between Figs. 9 and 10, it is seen that sialon ceramics rolls should dip also fast $u = 25$ mm/s rather than slowly $u = 2$ mm/s.
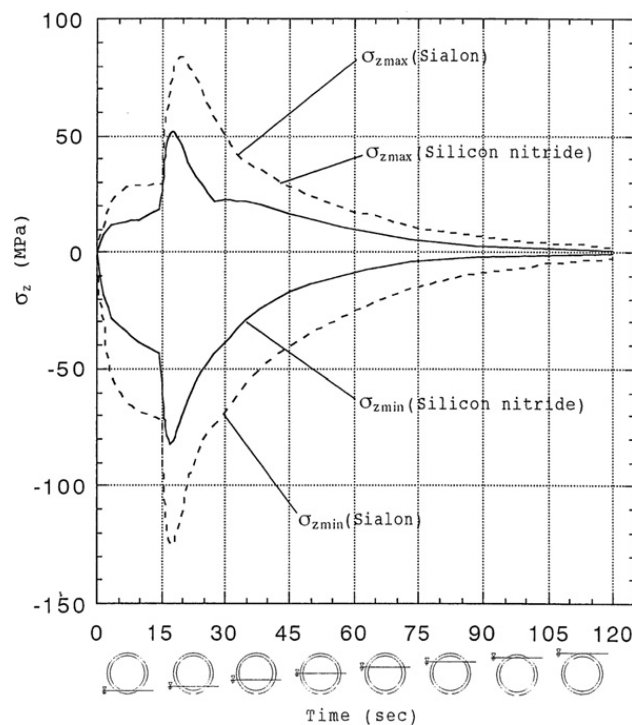

Fig. 14. σ_z vs. time relation for hollow cylinder made of special silicon nitride when the roll is preheated to 300 °C ($u = 2$ mm/s).

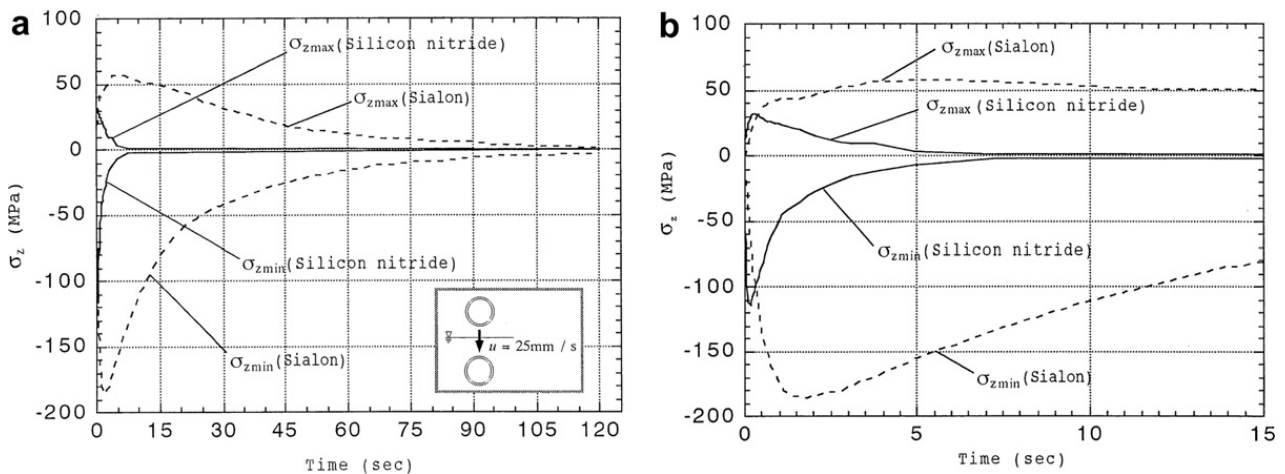Fig. 15. σ_z vs. time relation for hollow cylinder made of special silicon nitride when the roll is preheated to 300 °C ($u = 25$ mm/s)

4.6. Effect of preheat the ceramics roll to reduce thermal stress

Thermal stress may be reduced by heating ceramics rolls very slowly in a furnace by about 5 °C min to 300 °C before dipping the bath. Figs. 14 and 15 indicate the thermal stress σ_z when the hollow cylinder whose initial temperature is 300 °C. When the roll dips slowly, the maximum stress of special silicon nitride 52 MPa appearing at $t = 17$ s is lower than the one in Fig. 9 by 62% (see Figs. 14 and 9). Also the maximum stress of sialon 84 MPa appearing at $t = 19$ is lower than the one in Fig. 9 by 62%. When the roll dips fast, the maximum stress of special silicon nitride 32 MPa appearing at $t = 0.28$ s is lower than the one in Fig. 9 by 62% (see Figs. 15 and 10). From Figs. 14 and 15, it is also seen that the preheated ceramics roll should dip fast rather than slowly to reduce the thermal stress.

5. Conclusions

In the continuous galvanizing lines, the sink rolls and the support rolls are usually made of stainless steel. However, corrosion and abrasion arise on the roll surface only in a few weeks, and causing the deterioration of quality of plating. Although developing all-ceramics rolls as shown in Fig. 2 is most desirable, sometimes fracture occurs when the ceramic roll dips into molten metal. In this paper, therefore, how to reduce the thermal stress was considered when the all ceramics rolls are installed in molten metal bath using finite element method. The conclusions can be given in the following way.

(1) To reduce the thermal stress in hollow cylinders, they should dip into molten zinc fast $u = 25$ mm/s rather than slowly $u = 2$ mm/s. In other words, although in many continuous galvanizing lines hollow rolls are set slowly about $u = 2$ mm/s, that is not suitable for the thermal stress.
(2) On the other hand, for solid cylinders should dip into slowly in order to reduce the thermal stress.
(3) The thermal stress can be reduced by the use of the special silicon nitride by about 40%. This is because the thermal conductivity of this material is much higher than the one of other structural ceramics by 3.8 times [10].
(4) Thermal stress may be reduced by about 60% through heating all ceramics roll very slowly in a furnace by 5 °C/min to 300 °C before dipping the bath.

It should be noted that the ceramic rolls did behave in practice as predicted by the theory.

References

[1] Kaji Y, Iida Y, Nakagawa M, Okuuchi T, Kimura M. New Technologies for Continuous Galvanized Lines. Hitachi Technical Report, vol. 72(5); 1990. p. 429–36 [in Japanese].
[2] Adachi T, Tamura Y, Yoshioka T. Techniques of Automatic Operation in Continuous Galvanizing Line. Kawasaki Steel Technical Report, vol. 34; 1996. p. 18–25.
[3] Nishimura K, Katayama K, Kimura T, Yamaguchi T, Ito M. Newly Developed Techniques for Improving the Quality of Continuous Hotdip Plating Strips. Hitachi Technical Report, vol. 65(2); 1983. p. 121–6 [in Japanese].
[4] Takasugi T, Nogami S, Korenaga I. Application of sialon ceramics to the roll bearing in continuous galvanizing line. CAMP-ISIJ 2000;13:339 [in Japanese].
[5] Korenaga I. Sialon ceramics products used in molten aluminum. Sokeizai 1991;5:12–7 [in Japanese].
[6] Nogami S. Large Sialon Ceramics Product for Structural Use. Hitachi Metal Technical Report, vol. 15; 1999. p. 115–20 [in Japanese].
[7] Takasugi T, Nogami S. Rolls Used for Continuous Galvanizing Line. Japan Patent 2002-161347; 2002 [in Japanese].
[8] Harada Y, Komatsu K, Nomura N. Rolls Used for Continuous Galvanizing Line. Japan Patent 1991-63565; 1991 [in Japanese].
[9] Sakai J, Sobue M, Nakagawa Y. Rolls Used for Continuous Galvanizing Line and Plating System. Japan Patent 1993-271887; 1993 [in Japanese].

[10] Imamura T, Sobue M, Hamayoshi S. How to Produce Silicon Nitride Having High Thermal Conductivity and Circuit Board. Japan Patent 2002-293642; 2002 [in Japanese].

[11] Zukauskas A. Heat transfer from tubes in crossflow. In: Hartnett JP, Irvine Jr TF, editors. Advances in heat transfer, vol. 8. New York: Academic Press; 1972. p. 131.

[12] Editorial committee of JSME. Data of heat transfer. Tokyo: JSME; 1986. p. 61 [in Japanese].

[13] Editorial committee of JSME. Data of heat transfer. Tokyo: JSME; 1986. p. 323 [in Japanese].